Accepted Manuscript

DNA-hosted copper nanoclusters/graphene oxide based fluorescent biosensor for protein kinase activity detection

Mengke Wang, Zihan Lin, Qing Liu, Shan Jiang, Hua Liu, Xingguang Su

PII: S0003-2670(18)30094-1

DOI: 10.1016/j.aca.2018.01.029

Reference: ACA 235675

To appear in: *Analytica Chimica Acta*

Received Date: 10 November 2017

Revised Date: 10 January 2018

Accepted Date: 15 January 2018

Please cite this article as: M. Wang, Z. Lin, Q. Liu, S. Jiang, H. Liu, X. Su, DNA-hosted copper nanoclusters/graphene oxide based fluorescent biosensor for protein kinase activity detection, *Analytica Chimica Acta* (2018), doi: 10.1016/j.aca.2018.01.029.

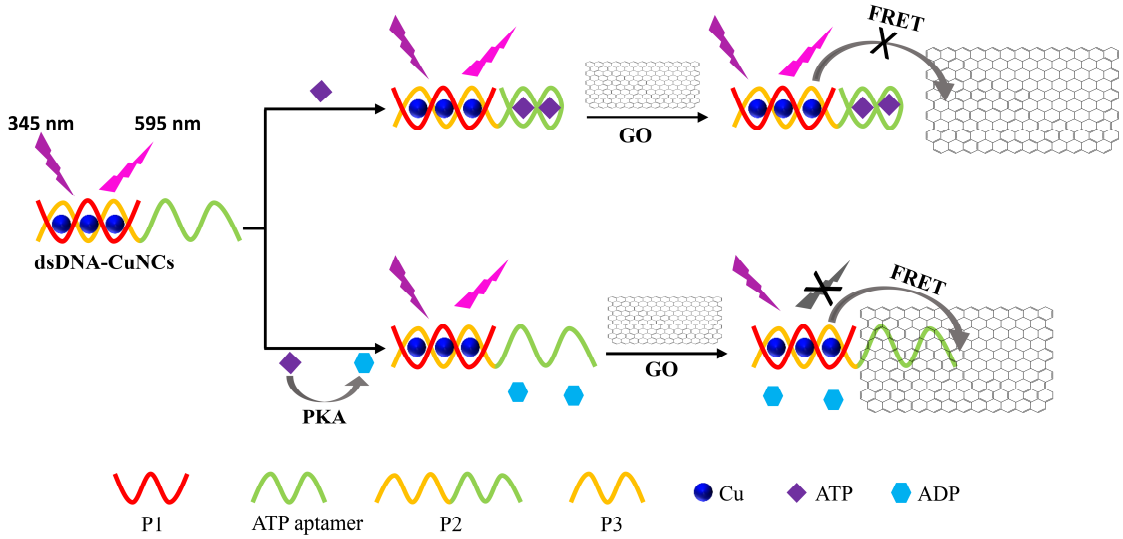

DNA-hosted copper nanoclusters/graphene oxide based fluorescent biosensor for protein kinase activity detection

Mengke Wang[a], Zihan Lin[b], Qing Liu[a], Shan Jiang[c], Hua Liu[a], Xingguang Su[a*]

[a] *Department of Analytical Chemistry, College of Chemistry, Jilin University, Changchun 130012, China*

[b] *Department of Chemistry and Chemical Engineering, Changchun University of Science and Technology, Changchun 130022, China*

[c] *State Key Laboratory of Supramolecular Structure and Materials, Jilin University, Changchun 130012, China*

*Corresponding author

Tel.: +86-431-85168352

E-mail address: suxg@jlu.edu.cn

Abstract

A novel fluorescent biosensor for protein kinase activity (PKA) detection was designed by applying double-strands DNA-hosted copper nanoclusters (dsDNA-CuNCs) and graphene oxide (GO). One DNA strand of the dsDNA consisted of two domains, one domain can hybridize with another complementary DNA strand to stabilize the fluorescent CuNCs and another domain was adenosine 5'-triphosphate (ATP) aptamer. ATP aptamer of the dsDNA-CuNCs would be spontaneously absorbed onto the GO surface through π-π stacking interactions. Thus GO can efficiently quench the fluorescence (FL) of dsDNA-CuNCs through fluorescence resonance energy transfer (FRET). In the present of ATP, ATP specifically combined with ATP aptamer to form ATP-ATP aptamer binding complexes, which had much less affinity to GO, resulting in the fluorescence recovery of the system. Nevertheless, in the presence of PKA, ATP could be translated into ADP and ADP could not combine with ATP aptamer resulting in the fluorescence quenching of dsDNA-CuNCs again. According to the change of the fluorescence signal, PKA activity could be successfully monitored in the range of 0.1 to 5.0 U mL^{-1} with a detection limit (LOD) of 0.039 U mL^{-1}. Besides, the inhibitory effect of H-89 on PKA activity was studied. The sensor was performed for PKA activity detection in cell lysates with satisfactory results.

Key words: dsDNA-CuNCs; Graphene oxide; Aptamer; PKA activity; Inhibitor

1. Introduction

Protein kinases, a class of biological enzyme, can catalyze phosphorylation of a peptide or protein substrate at threonine, serine or tyrosine via transferring a phosphate group from adenosine 5'-triphosphate (ATP) [1,2], regulating numerous cellular processes, and protein phosphorylation is one of the most vital posttranslational modifications [3]. Aberrant phosphorylation activity can lead to crucial diseases such as cancer and Alzheimer's disease [4-6]. Furthermore, protein kinases have been considered as important targets for drug development and disease detection [7,8]. Therefore, close monitoring and quantification of protein kinase activity is of crucial significance in terms of clinical diagnosis, targeted therapy and drug discovery.

Recently, many methods have been proposed for protein kinase activity assaying, such as electrochemistry [9-11], colorimetry [12,13], electrogenerated chemiluminescence (ELC) [14], fluorescence (FL) [15,16]. Based on possessing charming properties such as rapid response, wonderful sensitivity and operational simplicity, fluorescence methods draw more and more attentions. For example, Tan and his coworkers reported a sensitive affinity separation-based fluorescent method for protein kinase (PKA) activity detection [17]. In this assay, when PKA phosphorylated fluorescein isothiocyanate (FITC) labeled substrate peptide (S-peptide), specific adsorption between Zr^{4+}-immobilized nitrilotriacetic acid-coated magnetic nanoparticles (Zr-NTA MNPs) and phosphorylated peptides was triggered, and after magnetic separation processing, the fluorescence intensity of the solution had obvious changes. Qiu's group applied specially designed peptide templated gold nanoclusters (peptide-AuNCs) as an effective fluorescent probe for PKA activity detection based on the fact that phosphorylation of peptide by PKA protected the peptide-AuNCs from the digestion of carboxypeptidase Y (CPY) [18]. Nevertheless, these fluorescent methods require expensive raw materials, complex design processes, artificial

substrate peptides, specially designed enzymatic hydrolysis procedures and special fluorescent dyes, which significantly increases the experimental difficulty and outlay. Therefore, it is of extreme importance to establish simple, low cost and label-free methods for protein kinase activity detection.

Fluorescent noble metal nanoclusters (NCs), which was made up of several to tens of metal atoms with diameters below 2 nm, are of particular interest due to their excellent optical, physical and electronic properties [19,20]. Among these metal NCs, double-stranded DNA (dsDNA) templated copper nanoclusters (dsDNA-CuNCs) have attracted tremendous interest owing to the simple synthesis without rigorously controlled temperature, good water solubility, low toxicity, biocompatibility, and high specificity [21,22]. Recently, dsDNA-CuNCs have been wildly applied to detect biological enzymes [22], amino acids [23], lead ions [24] and so on.

Graphene oxide (GO), a single-atomic-layered two-dimensional carbon nanomaterial, has emerged as a fascinating nanomaterial for future high-tech applications owing to its high charge carrier mobilities, the electrical and thermal conductivity, combined with transparency and mechanical strength [25,26]. Biomolecules can be immobilized onto the GO surface through noncovalent methods due to the fact that planar structure of GO contains π electron structure and exhibits large specific surface area [27], which makes GO act as an efficient “nanoquencher” for the fluorophore via fluorescence resonance energy transfer (FRET) or non-radiative dipole-dipole coupling, attracting close attention in GO-based fluorescent biosensing [28-30]. Recently, many researches have reported that single-stranded DNA (ssDNA) can be adsorbed on the GO surface through π-π stacking interactions between the nucleobases and the GO sheet, and hydrogen bonding interaction between -OH or -COOH groups of GO and -OH or -NH_2 groups of ssDNA

[31,32], which results in the fluorescence quenching of energy donor adsorbed on GO surface through electron transfer (ET) or FRET while double-stranded DNA (dsDNA) or target molecule-aptamer DNA complexes having less surface effect can be removed from the GO surface more easily [33-35]. Hence, the optical biosensor based on coupling the fluorescent DNA templated metal nanoclusters with GO can be established.

Herein, we presented a novel fluorescent biosensor for PKA activity detection by applying the dsDNA-CuNCs and GO. As shown in Scheme 1, GO could absorb dsDNA-CuNCs onto its surface through the interactions with ATP aptamer sequence of dsDNA-CuNCs and quench the fluorescence of dsDNA-CuNCs through FRET. When ATP was added to the system of dsDNA-CuNCs, ATP combined with the ATP aptamer sequence of dsDNA-CuNCs to form ATP-ATP aptamer binding complexes, causing dsDNA-CuNCs far away from GO surface, and the fluorescence intensity of dsDNA-CuNCs recovered. After PKA addition, ATP could be translated into ADP by PKA, and ADP could not combine with ATP aptamer, resulting in the release of ATP aptamer to cause the fluorescence quenching of dsDNA-CuNCs again. Thus, the PKA activity could be effectively monitored based on the variation of fluorescence intensity. Compared with previous works, this strategy avoided tedious design and experimental processes, toxicity of organic reagents, extra costly enzymes and special fluorescent dyes, supplying a convenient, cheap and label-free sensing system for PKA activity detection.

Scheme 1

2. Experimental section

2.1. Reagents and instruments

$CuSO_4 \cdot 5H_2O$ and sodium ascorbate were obtained from Aladdin Reagent Co., Ltd. Protein kinase A (PKA, catalytic subunit from bovine heart), adenosine 5'-triphosphate (ATP) disodium salt hydrate, glucose oxidase (GOx), horseradish peroxidase (HRP), thrombin, tyrosinase (TYR), and N-[2[[3-(4-Brompophenyl)-2-propenyl]amino]ethyl]-5-isoquinolinesulfonamide (H-89) were bought from Sigma-Aldrich. Other inorganic reagents (analytically pure) were gotten from Beijing Chemical Co. and used as received without further purification. The water used throughout the whole experiment had a resistivity higher than 18 $M\Omega \cdot cm^{-1}$. All the oligonucleotides applied in this work were synthesized and purified by Sangon (Shanghai, China). Their sequences are as follows:

DNA strand P1: 5'-ATATATATATATACGGCAATTAATTAATTA-3'

DNA strand P2: 5'-TAATTAATTAATTGCCGTATATATATATAT**ACCTGGGGGAGTATTG CGGAGGAAGGT**-3'

DNA strand P3: 5'-TAATTAATTAATTGCCGTATATATATATAT-3'

The boldfaced letters in DNA strand P2 are the ATP aptamer sequence, and the DNA strand P1 is the complementary sequence of the underlined letters in P2 and DNA strand P3.

Fluorescence spectra were obtained by a RF-5301 PC spectrofluorophotometer (Shimadzu, Japan) equipped with a xenon lamp using right-angle geometry. Ultraviolet measurements were conducted on a Shimadzu UV-1700 UV-Visible spectrophotometer (Shimadzu Co., Kyoto, Japan). Transmission electron microscopy (TEM) was recorded through a Hitachi H-800 electron microscope at an acceleration voltage of 200 kV with a CCD camera. All pH assays were carried out using a PHS-3C pH meter (Tuopu Co., Hangzhou, China). All temperature assays were

accomplished through using a water bath.

2.2 Synthesis of fluorescent dsDNA-CuNCs

The fluorescent dsDNA-CuNCs were synthesized according to a modified synthetic report previously [23]. In brief, 8 μL DNA strand P1 (25 μM) and 8 μL DNA strand P2 (25 μM) were mixed together in 224 μL PBS solution (10 mM, pH = 7.4, containing 150 mM NaCl and 1 mM $MgCl_2$), and the mixture was incubated at ambient temperature for 30 min. After that, 150 μL sodium ascorbate (4.8 mM) and 10 μL $CuSO_4$ (5 mM) were added into the solution to give a final volume of 400 μL. After the system reacted for 10 min at ambient temperature, the fluorescent dsDNA-CuNCs were finally obtained.

2.3 Synthesis of graphene oxide

GO was prepared by a modified Hummer's method described previously [36,37]. Briefly, 2.0 g graphite powder was introduced into 12 mL H_2SO_4 (98%) which consisted of 2.5 g $K_2S_2O_8$ and 2.5 g P_2O_5. Next, the mixture solution was reacted at 80 °C for 4.5 h, and then diluted with 500 mL ultrapure water. The mixture was filtered and washed with ultrapure water to remove the residual acid, after that, the obtained product was dried at ambient conditions for one night. Subsequently, the pre-oxidation of graphite was stirred in 120 mL H_2SO_4 (98%), and then 15 g $KMnO_4$ was slowly added into the mixture when the temperature was kept above 20 °C. The obtained mixture was stirred at 35 °C for 0.5 h and 90 °C for another 1.5 h. After that, the mixture was diluted with 250 mL ultrapure water and then kept at 105 °C for 25 min. After the resulting mixture was equably stirred for 2 h, the reaction experiment was terminated with the addition of 700 mL ultrapure water and 20 mL H_2O_2 (30%). As for the purification of the product, the mixture was filtered and then washed with 1:10 1.1 M HCl aqueous solution-water lots of times. At last,

the product was ulteriorly purified through dialysis for 1 week for removing the remaining metal species. The obtained dispersion was centrifuged at 10,000 rpm (centrifugal force 6,820 g) in order to remove the unexfoliated GO. The supernatant solution was then collected and frozen dry. The GO powder was redispersed in water to obtain 1 mg mL^{-1} GO stock solution. The as-prepared GO stock solution (1 mg mL^{-1}) was stored at 4 °C prior for further application.

2.4 Detection of PKA activity and its inhibitor

For PKA activity measurement, 20 μL ATP (2.5 mM) and 10 μL different concentrations of PKA were mixed with 20 μL PBS solution (20 mM, pH = 7.4, containing 50 mM KCl and 10 mM $MgCl_2$) and the system was incubated at 37 °C for 1 h. Subsequently, 300 μL dsDNA-CuNCs were added into the mixture and the system reacted at ambient temperature for 10 min. Then, 50 μL GO (1 mg mL^{-1}) was added into the mixed system to give a final volume of 400 μL. After 8 min, the fluorescence spectra were recorded in the emission wavelength range of 500-670 nm with the excitation wavelength of 345 nm, and the excitation and emission slits were set at 5 nm and 10 nm respectively at room temperature.

For PKA inhibitor assay, the similar procedures were carried out as previously described, except that PKA was firstly pretreated with various concentrations of H-89 for 1h.

2.5 Detection of PKA in HepG-2 Cell Lysates

HepG-2 cells (1×10^6 cells) were cultured in Dulbecco's modified Eagle's medium (DMEM)/F-12 (1:1) supplemented with fetal bovine serum (10%) and were incubated under a humidified atmosphere containing CO_2 (5%) at 37 °C in a cell culture box for 3-4 days. After serum free medium replacing the culture medium, the cultured cells were centrifuged at 10,000 rpm (centrifugal force 6,820 g) to remove the nutrient solution, and then broken with an ultrasonic

liquid processor for 2 min. The HepG-2 cell lysates were centrifuged once more and ready for the following experiment. Subsequently, three different concentrations of PKA were added into the cell lysates to prepare the spiked cell lysate samples. For PKA activity measured in HepG-2 cell lysates, the same experiments were carried out except that the equal volume of above-prepared spiked cell lysate samples instead of the addition of pure PKA to the reaction system for investigation.

3. Results and discussion

3.1. Characterization of dsDNA-CuNCs and GO

It has been reported that through the reduction of low concentration of Cu^{2+} by AA, random dsDNA could act as efficient templates for the formation of CuNCs along with the fluorescence intensity, whereas random ssDNA had no ability to support the formation of CuNCs [38,39]. The dsDNA-CuNCs we synthesized were characterized through transmission electron microscopy (TEM), fluorescence (FL) spectroscopy and UV-vis absorption spectroscopy. The TEM image of dsDNA-CuNCs (Fig. 1A) revealed the clusters were well monodispersed and had an average diameter of 2 nm. As shown in Fig. 1B, the fluorescence spectra of dsDNA-CuNCs illustrated that the maximum fluorescence excitation and emission were 345 and 595 nm, respectively. The UV-vis absorption spectrum of dsDNA-CuNCs exhibited absorption bands at 345 nm, which was accordance with the excitation spectrum. The effect of Cu^{2+} concentration on the fluorescence intensity of dsDNA-CuNCs was studied. As seen in Fig. S1, with the increasing concentration of Cu^{2+}, the fluorescence intensity of dsDNA-CuNCs increased firstly and then decreased, and reached maximum at the Cu^{2+} concentration of 125 μM, which was due to that Cu^{2+} ions were more inclined to interact with the backbone phosphate negative groups by nonspecific electrostatic

attraction when the Cu^{2+} ions concentration was low [40] and the generated hydroxyl radicals destroyed the DNA double helix, causing the decreasing of the dsDNA templates when the Cu^{2+} ions concentration was higher [41]. Hence, the Cu^{2+} concentration 125 μM was chosen for the synthesis of dsDNA-CuNCs. As displayed in Fig. 1C, the UV-vis maximum absorption of GO was around 230 nm, and having a broad absorption band, which made GO act as an ideal energy acceptor for a variety of donors [33]. The FT-IR spectrum of GO (Fig. 1D) showed O-H stretching vibration of hydroxyl groups of GO at 3400 cm^{-1}. The emerging peaks at 1720 cm^{-1} and 1610 cm^{-1} were attributed to the vibrations of C=O and C=C bonds, respectively. The characteristic peak at 1400 cm^{-1} was associated with C-H stretching vibration, and the peak at 1110 cm^{-1} was attributed to C-O stretching. The results demonstrated the successful modification of carboxylic groups and hydroxyl groups on the GO surface.

Fig. 1

3.2. The strategy of biosensor design

The principle of the dsDNA-CuNCs/GO based sensing system for PKA activity detection was presented in Scheme 1, and dsDNA-CuNCs were used as fluorescent probes and combined with GO which possessed the superb fluorescence quenching ability to construct a novel PKA activity detection biosensor based on the FRET from donor dsDNA-CuNCs to acceptor GO. DNA strand P2 was specially designed, which consisted of two domains, where one domain (P3) hybridized with DNA strand P1 to stabilize fluorescent CuNCs and another domain was ATP aptamer sequence to form ATP-ATP aptamer binding complexes. In the absence of ATP, ATP aptamer

sequence of dsDNA-CuNCs would be spontaneously absorbed onto the GO surface through π-π stacking interactions between the nucleobases and the GO sheet, and hydrogen bonding interaction between -COOH or -OH groups of GO and -NH_2 or -OH groups of ssDNA [31,42]. Based on the interactions, the donor dsDNA-CuNCs were brought in close proximity to the acceptor GO surface resulting in the occurrence of FRET. With the addition of ATP to the system of dsDNA-CuNCs, ATP combined with ATP aptamer to form ATP-DNA binding complexes, which had much less affinity to GO, causing dsDNA-CuNCs far away from GO surface, resulting in the fluorescence recovery of the system [35]. DNA strand P1 was used to hybridize with P3 to stabilize CuNCs (dsDNA(P1-P3)-CuNCs), and as shown in Fig. S2, GO had less fluorescence quenching effect on dsDNA(P1-P3)-CuNCs, which indicated that totally complementary dsDNA had low binding affinity to GO, which was consistent with the previous report [33]. Meanwhile, PKA would translate ATP into ADP, and ADP had no competence to combine with ATP aptamer, so ATP aptamer sequence of dsDNA-CuNCs was released and absorbed onto the surface of GO again, which will lead to the fluorescence quenching of the system again. So the activity of PKA could be effectively monitored on the basis of the variation of fluorescence signal.

As shown in Fig. 2, the fluorescence intensity of dsDNA-CuNCs decreased to 36.6% of the original intensity in the presence of GO (125 μg mL^{-1}). When ATP, PKA or PKA/ATP was added to the dsDNA-CuNCs system, the fluorescence intensity of dsDNA-CuNCs had almost no changes. Furthermore, remarkable fluorescence increasing of dsDNA-CuNCs/GO system was observed when the dsDNA-CuNCs system was treated with ATP before the addition of GO, which indicated that the fluorescence increasing was as a consequence of the combine of ATP with ATP aptamer prohibiting the interaction between ATP aptamer and GO, which caused dsDNA-CuNCs far away

from GO. And the fluorescence intensity of dsDNA-CuNCs/ATP/GO system decreased when PKA was added into the dsDNA-CuNCs/ATP/GO system to translate ATP into ADP. All these results proved the possibility of the fluorescent assay for PKA activity detection.

Fig. 2

3.3 Optimization for PKA activity detection

In order to obtain optimal sensing performance for quantity analysis of PKA activity, the concentrations of GO and ATP, the incubation time between ATP and ATP aptamer sequence of dsDNA-CuNCs, the reaction time between the dsDNA-CuNCs and GO, the incubation temperature for ATP and ATP aptamer sequence of dsDNA-CuNCs and the incubation temperature for dsDNA-CuNCs and GO were investigated. The effect of the concentration of GO on the sensing system was shown in Fig. 3. It can be seen that the fluorescence intensity of dsDNA-CuNCs/GO system gradually decreased with the increasing concentration of GO and reached a plateau when the concentration of GO reached 125 μg mL^{-1}, which illustrated that ATP aptamer sequence of dsDNA-CuNCs was completely adsorbed on the GO surface when the GO concentration was over 125 μg mL^{-1}, and the fluorescence quenching percentage was approximately 63.4%, which provided a low background for the dsDNA-CuNCs/GO based sensing system. Therefore, 125 μg mL^{-1} GO was used in the further experiments. The effect of ATP concentration on the system of PKA activity detection was also studied. As displayed in Fig. S3, the fluorescence intensity of dsDNA-CuNCs/ATP/GO system obviously increased with the increasing concentration of ATP and reached a plateau when the concentration of ATP was higher

than 125 μM. Therefore, we chose 125 μM ATP in the subsequent experiments.

Fig. 3

In addition, the incubation time between ATP and ATP aptamer sequence of dsDNA-CuNCs was also optimized. As shown in Fig. S4, the fluorescence intensity of the dsDNA-CuNCs/ATP/GO system remarkably increased and reached the maximum within 10 min and then remained stable with time increasing. Therefore, we chose 10 min for the incubation time between ATP and ATP aptamer. The reaction time between dsDNA-CuNCs and GO was also investigated. From Fig. S5, it can be seen that the fluorescence intensity of the dsDNA-CuNCs/GO system dramatically decreased to the minimum within 8 min and then remained stable with more reaction time, which demonstrated that ATP aptamer sequence of dsDNA-CuNCs was rapidly adsorbed on the GO surface and GO quenched the fluorescence of dsDNA-CuNCs quickly. Thus, 8 min was selected as the optimal reaction time between dsDNA-CuNCs and GO.

The incubation temperature for ATP and ATP aptamer sequence of dsDNA-CuNCs was further studied. As shown in Fig. S6, the the fluorescence intensity of the dsDNA-CuNCs/ATP/GO system reached a maximum when the temperature was 25 °C. Therefore, 25 °C was chosen for the incubation temperature between ATP and ATP aptamer sequence of dsDNA-CuNCs. Besides, the incubation temperature between the dsDNA-CuNCs and GO were also optimized. As displayed in Fig. S7, the fluorescence intensity of dsDNA-CuNCs/GO system was the minimum when the temperature reached 25 °C. Thus, we selected 25 °C for the optimal reaction temperature between

the dsDNA-CuNCs and GO in the following experiments.

3.4. Detection of the PKA activity

Under optimized conditions, the determination of PKA activity was performed. The fluorescence emission spectra of dsDNA-CuNCs/ATP/PKA/GO system with different concentrations of PKA introduction were shown in Fig. 4. It can be seen that the fluorescence intensity of system gradually decreased with the increasing concentration of PKA. The inset in Fig. 4 displayed a good linearity between the fluorescence intensity ratio I/I_0 (I and I_0 were the fluorescence intensity of dsDNA-CuNCs/ATP/PKA/GO system in the presence and absence of PKA, respectively) and the PKA concentration in the range of 0.1-5.0 U mL^{-1}. The regression equation was $I/I_0 = 0.996 - 0.0866\ C_{PKA}$, U mL^{-1}, and the corresponding regression coefficient R^2 = 0.995. The detection limit (LOD = 3σ/k, where σ was the standard deviation of the blank signals (n = 11) of dsDNA-CuNCs/ATP/GO system and k was the slope of the fluorescence intensity versus PKA concentration) for PKA was 0.039 U mL^{-1}. A comparison between this method and other methods for PKA activity determination was listed in Table S1. From Table S1, it can be seen that our method showed a comparable quantification range and detection limit.

Fig. 4

3.5 Inhibitor assay

Enzyme inhibitor recognizes specific enzyme and efficiently reduces its catalytic activity, and many diseases are treated through using various enzyme inhibitors as drugs to block the intracellular signals, so the screening of potential inhibitor is of a great deal of significance in the

discovery of new drugs. In order to investigate whether this method has the potential application for protein kinase inhibitor screening, the inhibitor assay was conducted in the presence of a potential and cell-permeable PKA inhibitor H-89 with different concentrations [43]. From Fig. 5, it can be seen that the fluorescence intensity of the dsDNA-CuNCs/ATP/PKA/H-89/GO system obviously increased with the increasing concentration of H-89, which indicated that H-89 effectively inhibited the activity of PKA. And the FL intensity ratio I/I_0 (I and I_0 were the FL intensity of dsDNA-CuNCs/ATP/PKA/H-89/GO system in the presence and absence of H-89, respectively) increased with the increasing concentration of H-89 and reached a plateau when the concentration of H-89 was 1.00 μM, and the IC_{50} value (the half-maximal inhibitory concentration) for H-89 was detected to be 0.19 μM, which implied that the method provided a convenient way for protein kinase inhibitor monitoring.

Fig. 5

3.6 Selectivity study

The selectivity is considered as a significant parameter to evaluate a method performance to detect a specific species in complex biomedical samples. Therefore, the selectivity of our method with the treatment of different enzymes was further evaluated. Fig. 6 displayed the interference effects of 10 U mL^{-1} glucose oxidase (GOx), horseradish peroxidase (HRP), thrombin and tyrosinase (TYR) on the fluorescence intensity of dsDNA-CuNCs/ATP/GO system in comparison with 5 U mL^{-1} PKA. As shown in Fig. 6, the biosensor was not insensitive to potentially coexisting enzymes and selective to PKA in the presence of potentially coexisting enzymes, which indicated

that the fluorescent sensor performed satisfactory selectivity for PKA activity detection.

Fig. 6

3.5. PKA assay in HepG-2 Cell Lysates

For further investigating feasibility of this fluorescent biosensor for PKA activity detection in real samples, the determination of PKA activity in HepG-2 cell lysates was performed. The results which obtained by standard addition method were listed in Table 1. No PKA activity was detected in cell lysates before adding it, which agreed well with previously reports that there was no PKA activity in the cell lysate without drug stimulation [43,44]. From Table 1, it can be seen that the average recoveries of PKA in the cell lysates were in the range of 97.5-103.3%, and the relative standard deviation (RSD) was less than 3.0%, which indicated that the precision and accuracy of the method were satisfactory.

Table 1

4. Conclusion

A novel and convenient fluorescent biosensor for the detection of PKA activity and its inhibitor has been established. The biosensor was based on the FRET between dsDNA-CuNCs and GO and took the virtues of the strong interaction between ATP aptamer of dsDNA-CuNCs and GO, the superb quenching ability of GO, the specific aptamer-target recognition between ATP and ATP aptamer, and the good catalysis performance of PKA. In comparison with the previous reports for

PKA activity detection, this method avoided complex design process, laborious experimental procedure and expensive raw materials, providing a facile, low cost and sensitive biosensor for PKA activity determination. Besides, the developed method was performed to the detection of PKA activity in cell lysates and obtained satisfactory results.

Acknowledgments

This work was financial supported by the National Natural Science Foundation of China (No.21575048 and No. 21775052), the Science and Technology Development project of Jilin province, China (No. 20150204010GX).

References

[1] C.L. Wang, L.Y. Wei, C.J. Yuan, K.C. Hwang, Reusable amperometric biosensor for measuring protein tyrosine kinase activity, Anal Chem, 84 (2012) 971-977.

[2] K. Sun, Y. Chang, B. Zhou, X. Wang, L. Liu, Gold nanoparticles-based electrochemical method for the detection of protein kinase with a peptide-like inhibitor as the bioreceptor, Int J Nanomed, 12 (2017) 1905-1915.

[3] Y. Zhou, H. Yin, X. Li, Z. Li, S. Ai, H. Lin, Electrochemical biosensor for protein kinase A activity assay based on gold nanoparticles-carbon nanospheres, phos-tag-biotin and beta-galactosidase, Biosens. Bioelectron., 86 (2016) 508-515.

[4] P.J. Roberts, C.J. Der, Targeting the Raf-MEK-ERK mitogen-activated protein kinase cascade for the treatment of cancer, Oncogene, 26 (2007) 3291-3310.

[5] M. Flajolet, G. He, M. Heiman, A. Lin, A.C. Nairn, P. Greengard, Regulation of Alzheimer's disease amyloid-beta formation by casein kinase I, Proc Natl Acad Sci, 104 (2007) 4159-4164.

[6] L. Lin, Y. Liu, J. Yan, X. Wang, J. Li, Sensitive nanochannel biosensor for T4 polynucleotide kinase activity and inhibition detection, Anal Chem, 85 (2013) 334-340.

[7] S. Lapenna, A. Giordano, Cell cycle kinases as therapeutic targets for cancer, Nature Reviews Drug Discovery, 8 (2009) 547-566.

[8] G.B. Manoharan, E. Enkvist, A. Uri, Combining chemical and genetic approaches for development of responsive FRET-based sensor systems for protein kinases, Biophys Chem, 211 (2016) 39-48.

[9] L. Liu, C. Cheng, Y. Chang, H.Y. Ma, Y.Q. Hao, Two sensitive electrochemical strategies for the detection of protein kinase activity based on the 4-mercaptophenylboronic acid-induced in situ

assembly of silver nanoparticles, Sensor Actuat B-chem, 248 (2017) 178-186.

[10] M. Wang, G.X. Wang, F.N. Xiao, Y. Zhao, K. Wang, X.H. Xia, Sensitive label-free monitoring of protein kinase activity and inhibition using ferric ions coordinated to phosphorylated sites as electrocatalysts, Chem Commun, 49 (2013) 8788-8790.

[11] Z. Wang, N. Sun, Y. He, Y. Liu, J. Li, DNA assembled gold nanoparticles polymeric network blocks modular highly sensitive electrochemical biosensors for protein kinase activity analysis and inhibition, Anal Chem, 86 (2014) 6153-6159.

[12] J. Zhou, X. Xu, X. Liu, H. Li, Z. Nie, M. Qing, Y. Huang, S. Yao, A gold nanoparticles calorimetric assay for label-free detection of protein kinase activity based on phosphorylation protection against exopeptidase cleavage, Biosens. Bioelectron., 53 (2014) 295-300.

[13] S. Sun, H. Shen, C. Liu, Z. Li, Phosphorylation-regulated crosslinking of gold nanoparticles: a new strategy for colorimetric detection of protein kinase activity, Analyst, 140 (2015) 5685-5691.

[14] S. Xu, Y. Liu, T. Wang, J. Li, Highly sensitive electrogenerated chemiluminescence biosensor in profiling protein kinase activity and inhibition using gold nanoparticle as signal transduction probes, Anal Chem, 82 (2010) 9566-9572.

[15] G. Lu, P. Tan, C. Lei, Z. Nie, Y. Huang, S. Yao, Fluorescent detection of protein kinase based on positively charged gold nanoparticles, Talanta, 128 (2014) 360-365.

[16] W. Song, R.-P. Liang, Y. Wang, L. Zhang, J.-D. Qiu, Gold nanoclusters-based dual-emission ratiometric fluorescence probe for monitoring protein kinase, Sensor Actuat B-chem, 226 (2016) 144-150.

[17] P. Tan, C. Lei, X. Liu, M. Qing, Z. Nie, M. Guo, Y. Huang, S. Yao, Fluorescent detection of

protein kinase based on zirconium ions-immobilized magnetic nanoparticles, Anal Chim Acta, 780 (2013) 89-94.

[18] W. Song, R.P. Liang, Y. Wang, L. Zhang, J.D. Qiu, Green synthesis of peptide-templated gold nanoclusters as novel fluorescence probes for detecting protein kinase activity, Chem Commun, 51 (2015) 10006-10009.

[19] I. Diez, M. Pusa, S. Kulmala, H. Jiang, A. Walther, A.S. Goldmann, A.H.E. Muller, O. Ikkala, R.H.A. Ras, Color tunability and electrochemiluminescence of silver nanoclusters, Angew Chem Int Ed, 48 (2009) 2122-2125.

[20] L. Shang, S. Dong, G.U. Nienhaus, Ultra-small fluorescent metal nanoclusters: synthesis and biological applications, Nano Today, 6 (2011) 401-418.

[21] X. Jia, J. Li, L. Han, J. Ren, X. Yang, E. Wang, DNA-hosted copper nanoclusters for fluorescent identification of single nucleotide polymorphisms, Acs Nano, 6 (2012) 3311-3317.

[22] R. Hu, Y.-R. Liu, R.-M. Kong, M.J. Donovan, X.-B. Zhang, W. Tan, G.-L. Shen, R.-Q. Yu, Double-strand DNA-templated formation of copper nanoparticles as fluorescent probe for label free nuclease enzyme detection, Biosens. Bioelectron., 42 (2013) 31-35.

[23] Y.-R. Liu, R. Hu, T. Liu, X.-B. Zhang, W. Tan, G.-L. Shen, R.-Q. Yu, Label-free dsDNA-Cu NPs-based fluorescent probe for highly sensitive detection of L-histidine, Talanta, 107 (2013) 402-407.

[24] J.H. Chen, J. Liu, Z.Y. Fang, L.W. Zeng, Random dsDNA-templated formation of copper nanoparticles as novel fluorescence probes for label-free lead ions detection, Chem Commun, 48 (2012) 1057-1059.

[25] S. Eigler, A. Hirsch, Chemistry with graphene and graphene oxide-challenges for synthetic

chemists, Angew Chem Int Ed, 53 (2014) 7720-7738.

[26] D. Chen, H. Feng, J. Li, Graphene oxide: preparation, functionalization, and electrochemical applications, Chem Rev, 112 (2012) 6027-6053.

[27] S. Li, Y. Fu, X. Ma, Y. Zhang, Label-free fluorometric detection of chymotrypsin activity using graphene oxide/nucleic-acid-stabilized silver nanoclusters hybrid materials, Biosens. Bioelectron., 88 (2017) 210-216.

[28] Y. Li, F.P. Shi, N. Cai, X.G. Su, A biosensing platform for sensitive detection of concanavalin A based on fluorescence resonance energy transfer from CdTe quantum dots to graphene oxide, New J Chem, 39 (2015) 6092-6098.

[29] C.H. Lu, H.H. Yang, C.L. Zhu, X. Chen, G.N. Chen, A graphene platform for sensing biomolecules, Angew Chem Int Ed, 48 (2009) 4785-4787.

[30] Y. Wang, L. Tang, Z. Li, Y. Lin, J. Li, In situ simultaneous monitoring of ATP and GTP using a graphene oxide nanosheet-based sensing platform in living cells, Nat Protoc, 9 (2014) 1944-1955.

[31] Y. Guo, L. Deng, J. Li, S. Guo, E. Wang, S. Dong, Hemin-graphene hybrid nanosheets with intrinsic peroxidase-like activity for label-free colorimetric detection of single-nucleotide polymorphism, Acs Nano, 5 (2011) 1282-1290.

[32] Y. Wang, Z. Li, T.J. Weber, D. Hu, C.-T. Lin, J. Li, Y. Lin, In situ live cell sensing of multiple nucleotides exploiting DNA/RNA aptamers and graphene oxide nanosheets, Anal Chem, 85 (2013) 6775-6782.

[33] Y.-D. Ye, L. Xia, D.-D. Xu, X.-J. Xing, D.-W. Pang, H.-W. Tang, DNA-stabilized silver nanoclusters and carbon nanoparticles oxide: A sensitive platform for label-free fluorescence

turn-on detection of HIV-DNA sequences, Biosens. Bioelectron., 85 (2016) 837-843.

[34] X. Liu, F. Wang, R. Aizen, O. Yehezkeli, I. Willner, Graphene oxide/nucleic-acid-stabilized silver nanoclusters: functional hybrid materials for optical aptamer sensing and multiplexed analysis of pathogenic DNAs, J Am Chem Soc, 135 (2013) 11832-11839.

[35] Y. Wang, Z.H. Li, D.H. Hu, C.T. Lin, J.H. Li, Y.H. Lin, Aptamer/graphene oxide nanocomplex for in situ molecular probing in living cells, J Am Chem Soc, 132 (2010) 9274-9276.

[36] Y. Xu, H. Bai, G. Lu, C. Li, G. Shi, Flexible graphene films via the filtration of water-soluble noncovalent functionalized graphene sheets, J Am Chem Soc, 130 (2008) 5856-+.

[37] H. Dong, W. Gao, F. Yan, H. Ji, H. Ju, Fluorescence resonance energy transfer between quantum dots and graphene oxide for sensing biomolecules, Anal Chem, 82 (2010) 5511-5517.

[38] A. Rotaru, S. Dutta, E. Jentzsch, K. Gothelf, A. Mokhir, Selective dsDNA-templated formation of copper nanoparticles in solution, Angew Chem Int Ed, 49 (2010) 5665-5667.

[39] X. Mao, S. Liu, C. Yang, F. Liu, K. Wang, G. Chen, Colorimetric detection of hepatitis B virus (HBV) DNA based on DNA-templated copper nanoclusters, Anal Chim Acta, 909 (2016) 101-108.

[40] V. Andrushchenko, J.H. van de Sande, H. Wieser, Vibrational circular dichroism and IR absorption of DNA complexes with Cu2+ ions, Biopolymers, 72 (2003) 374-390.

[41] C.F. Monson, A.T. Woolley, DNA-templated construction of copper nanowires, Nano Lett, 3 (2003) 359-363.

[42] H. Chang, L. Tang, Y. Wang, J. Jiang, J. Li, Graphene fluorescence resonance energy transfer aptasensor for the thrombin detection, Anal Chem, 82 (2010) 2341-2346.

[43] C. Shen, X. Xia, S. Hu, M. Yang, J. Wang, Silver nanoclusters-based fluorescence assay of

protein kinase activity and inhibition, Anal Chem, 87 (2015) 693-698.

[44] X. Xu, X. Liu, Z. Nie, Y. Pan, M. Guo, S. Yao, Label-free fluorescent detection of protein kinase activity based on the aggregation behavior of unmodified quantum dots, Anal Chem, 83 (2011) 52-59.

Captions:

Scheme 1 Schematic illustration of the fluorescent biosensor for PKA activity detection.

Fig. 1 (A) TEM image of dsDNA-CuNCs (scale bar: 10 nm). (B) UV-vis absorption spectrum (red line) and FL excitation (black line) and emission (blue line) spectra of dsDNA-CuNCs. The inset showed the photograph of aqueous solution of dsDNA-CuNCs obtained under 365 nm UV irradiation. (C) UV-vis absorption spectrum of GO. (D) FT-IR spectrum of GO.

Fig. 2 FL spectra of dsDNA-CuNCs, dsDNA-CuNCs/ATP, dsDNA-CuNCs/PKA, dsDNA-CuNCs/ATP/PKA, dsDNA-CuNCs/GO, dsDNA-CuNCs/ATP/GO, dsDNA-CuNCs/PKA/GO and dsDNA-CuNCs/ATP/PKA/GO system, respectively. Conditions: 300 μL dsDNA-CuNCs, 125 μM ATP, 5.0 U mL^{-1} PKA ,125 μg mL^{-1} GO.

Fig. 3 FL spectra of dsDNA-CuNCs/GO system in the presence of different concentrations of GO, from top to bottom: 0, 10, 25, 62.5, 85, 100, 125, 150 and 180 μg mL^{-1}, respectively. The inset was the FL quenching ratio I/I_0 versus the concentration of GO. I and I_0 were the FL intensity of the dsDNA-CuNCs/GO system the in the presence and absence of GO. Conditions: 300 μL dsDNA-CuNCs. The error bars were obtained from three parallel test results.

Fig. 4 Normalized FL spectra of dsDNA-CuNCs/ATP/PKA/GO system in the presence of different concentrations of PKA, from top to bottom: 0, 0.1, 0.3, 0.5, 1.0, 2.0, 3.0, 4.0. 5.0 and 6.0 U mL^{-1}, respectively. Normalized FL spectra of dsDNA-CuNCs/ATP/PKA/GO system were obtained via dividing by the maximum (the FL emission intensity of the system in the absence of PKA). The insert was the linearity of the relative FL intensity I/I_0 versus and PKA concentration. I and I_0 were the FL intensity of dsDNA-CuNCs/ATP/PKA/GO system in the presence and absence of PKA, respectively. Conditions: 300 μL dsDNA-CuNCs, 125 μM ATP, 125 μg mL^{-1} GO. The error bars

were obtained from three parallel test results.

Fig. 5 Normalized FL spectra of dsDNA-CuNCs/ATP/PKA/H-89/GO system in the presence of different concentrations of H-89, from bottom to top: 0, 0.03, 0.06, 0.08, 0.10, 0.20, 0.30, 0.55, 0.70, 0.90, 1.00 and 1.30 μM, respectively. Normalized FL spectra of dsDNA-CuNCs/ATP/PKA/H-89/GO system were obtained via dividing by the minimum (the FL emission intensity of the system in the absence of H-89). The insert was the relationship between the FL intensity ratio I/I_0 of dsDNA-CuNCs/ATP/PKA/H-89/GO system and H-89 concentration. I and I_0 were the FL intensity of dsDNA-CuNCs/ATP/PKA/H-89/GO system in the presence and absence of H-89, respectively. Conditions: 300 μL dsDNA-CuNCs, 125 μM ATP, 125 μg mL^{-1} GO, 5.0 U mL^{-1} PKA. The error bars were obtained from three parallel test results.

Fig. 6 The selectivity of the method for PKA activity detection. The concentration of PKA was 5.0 U mL^{-1}, and GOx, HRP, thrombin and TYR concentrations were both 10.0 U mL^{-1}. I and I_0 were the FL intensity of dsDNA-CuNCs/ATP/GO system in the presence and absence of enzyme, respectively. Conditions: 300 μL dsDNA-CuNCs, 125 μM ATP, 125 μg mL^{-1} GO. The error bars were obtained from three parallel test results.

Table 1 Determination of PKA in HepG-2 cell lysates

Table 1 Determination of PKA in HepG-2 cell lysates

Sample	PKA added ($U\ mL^{-1}$)	PKA founded ($U\ mL^{-1}$)	Recovery (%)	RSD (n = 3, %)
0	0	-	-	-
1	0.4	0.39	97.50	1.43
2	1.5	1.55	103.3	2.15
3	3.5	3.61	103.1	2.99

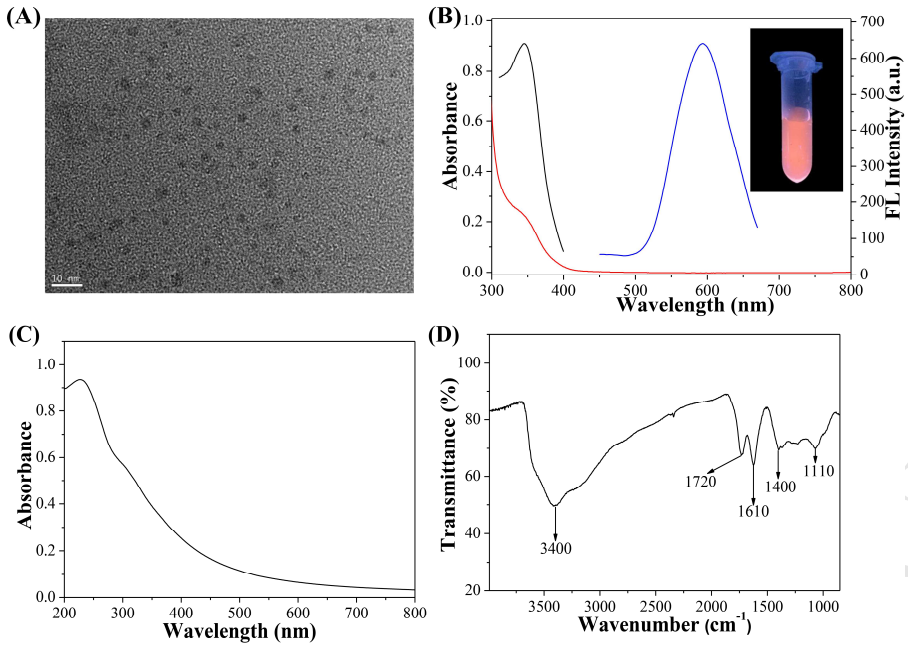

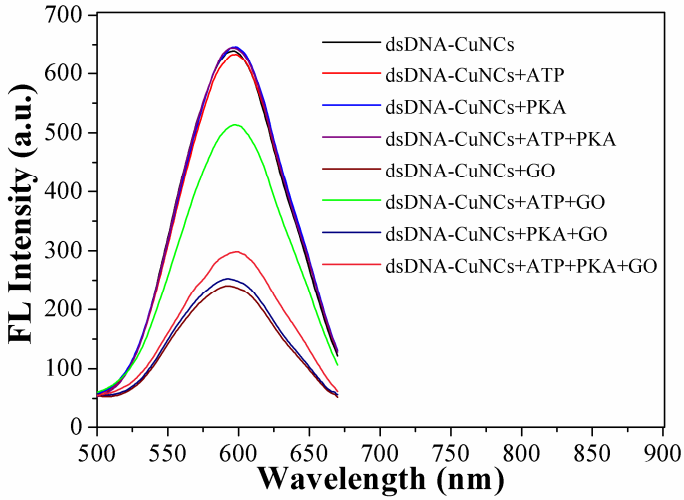

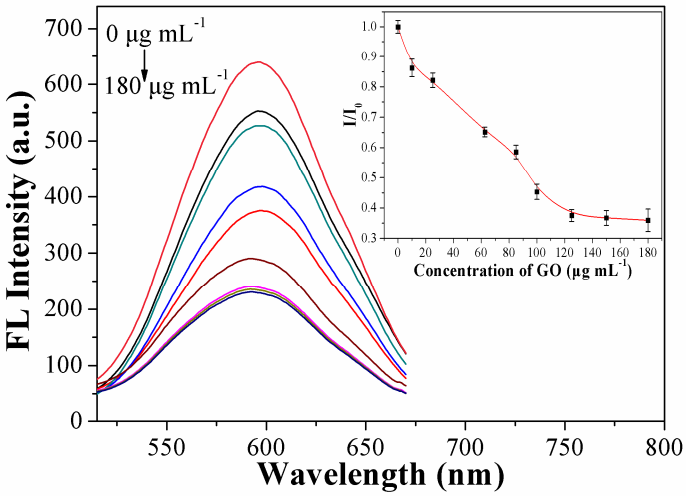

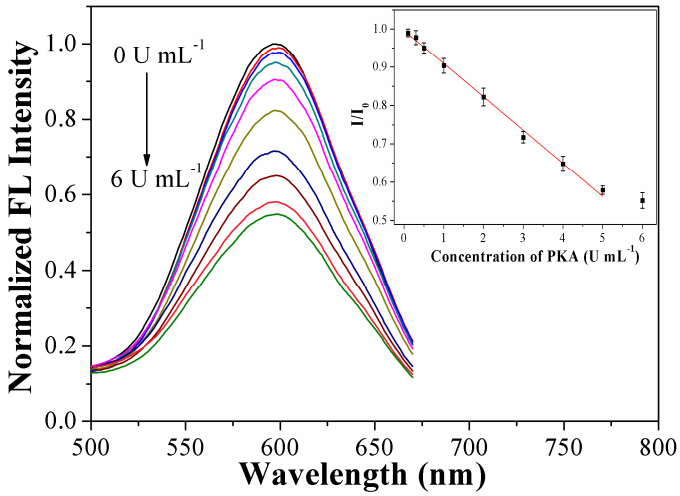

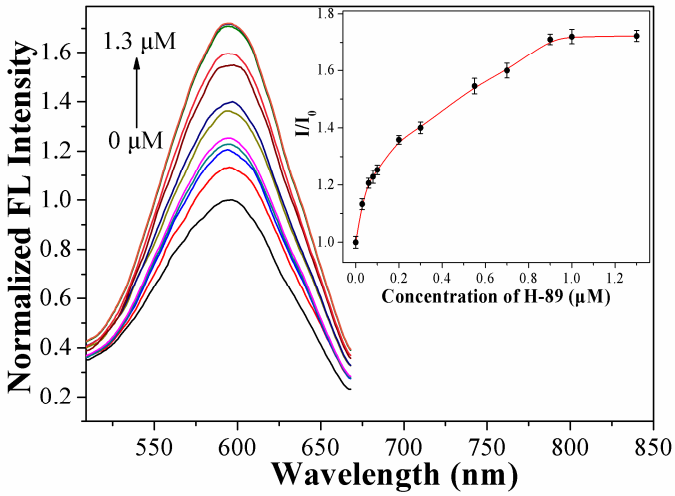

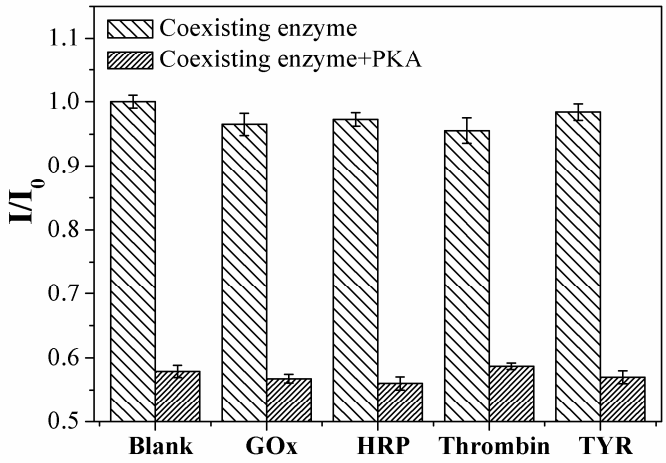

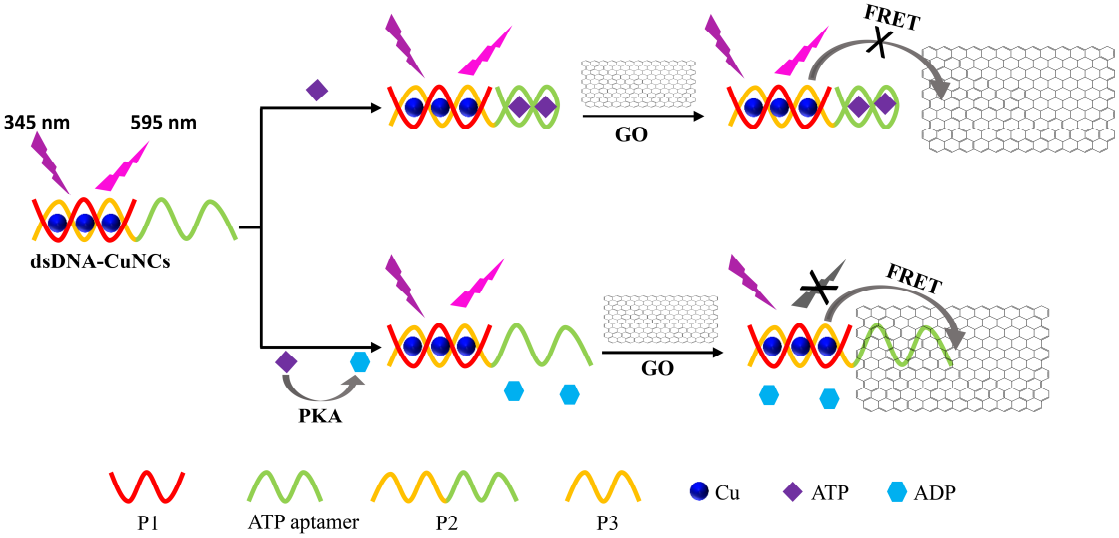

Highlights:

► A novel biosensor for convenient detection of PKA activity and its inhibitor was developed.

► The affinity of ATP aptamer sequence of dsDNA-CuNCs to GO caused the FRET.

► ATP broke the affinity of ATP aptamer to GO by forming ATP-ATP aptamer complexes.

► ATP aptamer was released and absorbed onto GO as soon as PKA translated ATP into ADP.

► The biosensor was performed for PKA detection in cell lysates with satisfactory results.